Cell

Resource

Cell-Cell Communication between Malaria-Infected Red Blood Cells via Exosome-like Vesicles

Neta Regev-Rudzki,[1,2,6] Danny W. Wilson,[1,2,6] Teresa G. Carvalho,[1,2,7] Xavier Sisquella,[1,2] Bradley M. Coleman,[3,4] Melanie Rug,[1,2,8] Dejan Bursac,[1,2] Fiona Angrisano,[1,2] Michelle Gee,[5] Andrew F. Hill,[3,4] Jake Baum,[1,2] and Alan F. Cowman[1,2,*]

[1]Division of Infection and Immunity, the Walter and Eliza Hall Institute of Medical Research, Parkville, Victoria 3052, Australia
[2]Department of Medical Biology
[3]Department of Biochemistry and Molecular Biology
[4]Bio21 Molecular Science and Biotechnology Institute
[5]School of Chemistry
The University of Melbourne, Melbourne, Victoria 3010, Australia
[6]These authors contributed equally to this work
[7]Present address: Department of Microbiology, Monash University, Clayton, Victoria 3168, Australia
[8]Present address: Centre for Advanced Microscopy, The Australian National University, Canberra, Australian Capital Territory 0200, Australia
*Correspondence: cowman@wehi.edu.au
http://dx.doi.org/10.1016/j.cell.2013.04.029

SUMMARY

Cell-cell communication is an important mechanism for information exchange promoting cell survival for the control of features such as population density and differentiation. We determined that *Plasmodium falciparum*-infected red blood cells directly communicate between parasites within a population using exosome-like vesicles that are capable of delivering genes. Importantly, communication via exosome-like vesicles promotes differentiation to sexual forms at a rate that suggests that signaling is involved. Furthermore, we have identified a *P. falciparum* protein, PfPTP2, that plays a key role in efficient communication. This study reveals a previously unidentified pathway of *P. falciparum* biology critical for survival in the host and transmission to mosquitoes. This identifies a pathway for the development of agents to block parasite transmission from the human host to the mosquito.

INTRODUCTION

Cell-cell communication and cooperative motility are well known in multicellular eukaryotes and include tissue morphogenesis, wound healing, and tumor metastases. Direct communication between mammalian cells occurs either by the transfer of information through microvesicles or physical connection through nanotubes (Belting and Wittrup, 2008; Gerdes and Carvalho, 2008). Extracellular vesicles (EVs) are small cellular particles of 30–400 nm, and their release is highly conserved in biology (reviewed in Delabranche et al., 2012). EVs are divided into microparticles (MPs), microvesicles (MVs) and exosomes on the basis of size and the cell compartment from which they originate. MPs (100–400 nm) are released by the vesiculation of plasma membranes, whereas exosomes (30–150 nm) originate from multivesicular bodies (MVBs) derived from late endosomes (Johnstone et al., 1987). Exosomes and MPs are involved in the transfer of biologically active molecules for the induction of phenotypic changes (Belting and Wittrup, 2008; Coleman et al., 2012; Ratajczak et al., 2006). In malaria, MPs are released from infected red blood cells (RBCs) and activate endothelium at the blood-brain barrier, exacerbating inflammation (Combes et al., 2005; Campos et al., 2010; Nantakomol et al., 2011).

Although cell-cell communication and social behavior is established in many eukaryotes and prokaryotes (Bassler and Losick, 2006; Dubey and Ben-Yehuda, 2011; Record et al., 2011), there is less known for parasitic protozoa (Lopez et al., 2011; Rupp et al., 2011). Protozoan parasites are responsible for major diseases, including malaria, caused by the genus *Plasmodium*. *P. falciparum* and *P. vivax* are responsible for most clinical cases of malaria in humans. These vector-born parasites cycle between mosquitoes and humans and, in both contexts, are faced with an unstable and hostile environment. To ensure survival and transmission, the malaria parasite must infect and survive in the human host and differentiate into sexual forms (gametocytes) that are competent for transmission to mosquitoes. The molecular mechanisms for commitment to gametocytogenesis, a "once in a life cycle" decision, are obscure in *Plasmodium* biology (reviewed in Alano, 2007).

In the protozoan parasite *Trypanosoma brucei*, which is responsible for sleeping sickness, a density-sensing mechanism activates the differentiation of proliferative slender cells to stumpy forms through the release of stumpy induction factor (STI) (MacGregor et al., 2011; Reuner et al., 1997; Vassella et al., 1997). Stumpy forms are committed to cell-cycle arrest in the host, which limits population density, and are competent for transmission to the tsetse fly. This quorum-sensing-like mechanism provides a

means for *T. brucei* to enhance vector transmission and prolong survival in the host (MacGregor et al., 2011).

It would be a major advantage for *Plasmodium* parasites, such as *P. falciparum*, to communication during blood-stage infection in order to enable populations to react to changing conditions in the host. To date, no study has provided direct evidence for its existence. Here, we demonstrate cell-cell communication between *P. falciparum* parasites through exosome-like vesicles that promote differentiation to sexual forms.

RESULTS

Communication between *P. falciparum* Cells Mediates DNA-Dependent Transfer of Drug Resistance and Fluorescence

To determine whether *P. falciparum*-infected RBCs communicate and transfer information, we used strains expressing different drug resistance cassettes and fluorescent proteins as markers. The parasite line 3D7edhfr^{GFP} has an episomal (e) plasmid expressing *human dihydrofolate reductase* (*dhfr*), conferring resistance to WR99210 (WR), and green fluorescent protein (GFP) (Boddey et al., 2010). A second line, CS2eBsd^{GFP}, contains an episomal (e) plasmid expressing blasticidin deaminase (Bsd), conferring resistance to blasticidin-S (Bs), and GFP (Ataíde et al., 2010). Parasite lines were cocultured in Bs+WR and, after initial cell death, expected because of the presence of both drugs, parasites grew to high parasitaemia within 5 days (Figures 1A and 1B). In contrast, when CS2eBsd^{GFP} or 3D7edhfr^{GFP} (parental lines) were cultured alone in both drugs, no parasites survived.

We tested other *P. falciparum* lines to determine whether they transferred drug resistance between cells. The WR-resistant CS2idhfr^{920} has an integrated (i) copy of *hdhfr* and was cocultured with Bs-resistant CS2eBsd^{GFP} in Bs+WR with ring-stage parasites observed after 5 days (Figure 1C). To test whether this was due to the release of plasmid into supernatants or uptake by parasitized RBCs, we added CS2idhfr^{920} to RBCs electroporated with a plasmid conferring Bs resistance (Figure 1C). Typically for this method of *P. falciparum* transfection, parasites are observed at 21 days (Fidock and Wellems, 1997). However, when plasmid-loaded RBCs were incubated with CS2idhfr^{920}, no ring-stage parasites were obtained after 5 days on Bs. Additionally, we added plasmid encoding a *bsd* gene to CS2idhfr^{920} parasites, and, again, no ring-stage parasites were detected after 5 days on Bs. Therefore, *P. falciparum* lines can rescue parasite growth, under drug selection, when cocultured, and this was not through the uptake of plasmid DNA released during normal growth.

If drug resistance genes were transferred to cells in the population via cell-cell communication, then fluorescent proteins encoded on the plasmid should be expressed. 3D7idhfr^{mCh} expresses mCherry in the nucleus (Volz et al., 2010), whereas CS2eBsd^{GFP} expresses GFP in the cytoplasm (Figure 1D) (Ataíde et al., 2010). We detected dual-colored (red nucleus and green cytoplasm) parasites after 5 days of coculture for CS2eBsd^{GFP}+3D7idhfr^{mCh} with Bs+WR (Figure 1D). To test whether the transfer of GFP or mCherry expression between parasites resulted from plasmid transfer, we used fluorescence in situ hybridization (FISH) to detect *bsd* (CS2eBsd^{GFP}) and *hdhfr* (3D7edhfr^{GFP}) genes in cocultured CS2eBsd^{GFP}+3D7edhfr^{GFP} parasites with Bs+WR (Figure 1E). In the coculture experiments analyzed by FISH, 100% of the parasites were positive for both *hdhfr* and *bsd* genes, confirming the transfer of an episomal plasmid. In contrast, the parental parasites were positive for only the endogenous drug resistance marker.

DNA-dependent transfer was confirmed by PCR of 3D7idhfr^{mCh}+CS2eBsd^{GFP} in Bs+WR (Figure 1F). The genes *hdhfr* and *mcherry* were present in 3D7idhfr^{mCh}, and, conversely, *bsd* and *gfp* were detected in CS2eBsd^{GFP}, as expected for parental lines. When 3D7idhfr^{mCh} and CS2eBsd^{GFP} were cocultured in Bs+WR, *hdhfr*, *mcherry*, *bsd*, and *gfp* genes were detected. This was not due to remnant genomic DNA (gDNA) from dead or dying cells, given that no genes were detected by PCR for 3D7idhfr^{mCh} and CS2eBsd^{GFP} parental lines cultured separately in Bs+WR (Figure 1F). Altogether, these data show that *P. falciparum* parasites can transfer information between cells in a population.

Parasite Communication Is Mediated by Factors Released by *P. falciparum*-Infected RBCs

To determine whether communication between *P. falciparum*-infected RBCs required cell contact, we used transwells to physically separate parasites in culture. We established that *P. falciparum* parasites could not pass through 400 nm pore transwell membranes. We separated 3D7edhfr^{GFP} and CS2eBsd^{GFP} in transwells with Bs+WR and assessed ring-stage parasitaemia after 5 days (Figure 2A). 3D7edhfr^{GFP} only survived in either the insert or bottom of the transwells when CS2eBsd^{GFP} was present in the opposite chamber. Interestingly, when placing the two parasite lines in different compartments of the transwell, the directionality of transfer was toward 3D7edhfr^{GFP} and not CS2eBsd^{GFP}, implying it was the drug selection cassette (*bsd*) and not the episomal plasmid, per se, that was determining the direction of transfer. The predominance of episomal *bsd* plasmid transfer was most likely because Bs inhibits the ring and early trophozoite stages (see Figure S1 available online), whereas WR inhibits later in the life cycle (Dieckmann and Jung, 1986). In these experiments, we added both drugs at ring stages, and, below, we show that the ring stage is critical for cell-cell communication.

Experiments with 3D7idhfr^{mCh} and CS2eBsd^{GFP} gave similar results with Bs drug resistance transferred to 3D7idhfr^{mCh} (Figure 2B). In related experiments, plasmid transfer from CS2eBsd^{GFP} to a second integrated line, CS2idhfr^{920}, was confirmed by PCR amplification of *hdhfr* and *gfp* genes in coculture transwells containing CS2idhfr^{920} after the removal of CS2eBsd^{GFP} in inserts (Figure 2C). Therefore, factors are released into supernatants that carry a DNA plasmid through a 400 nm pore in order to communicate with *P. falciparum*-infected RBCs. This demonstrates that communication between *P. falciparum* parasites does not require direct cell-cell contact and occurs over long distances.

Next, we exploited transwells to study whether DNA carrier factors present in cocultured media were stable and could "rescue" a drug resistance phenotype. Increasing volumes of 3D7edhfr^{GFP}+
CS2eBsd^{GFP} parasites were cultured in transwell inserts with Bs+WR (Figure 2D). After 24 hr of coculture, the insert was

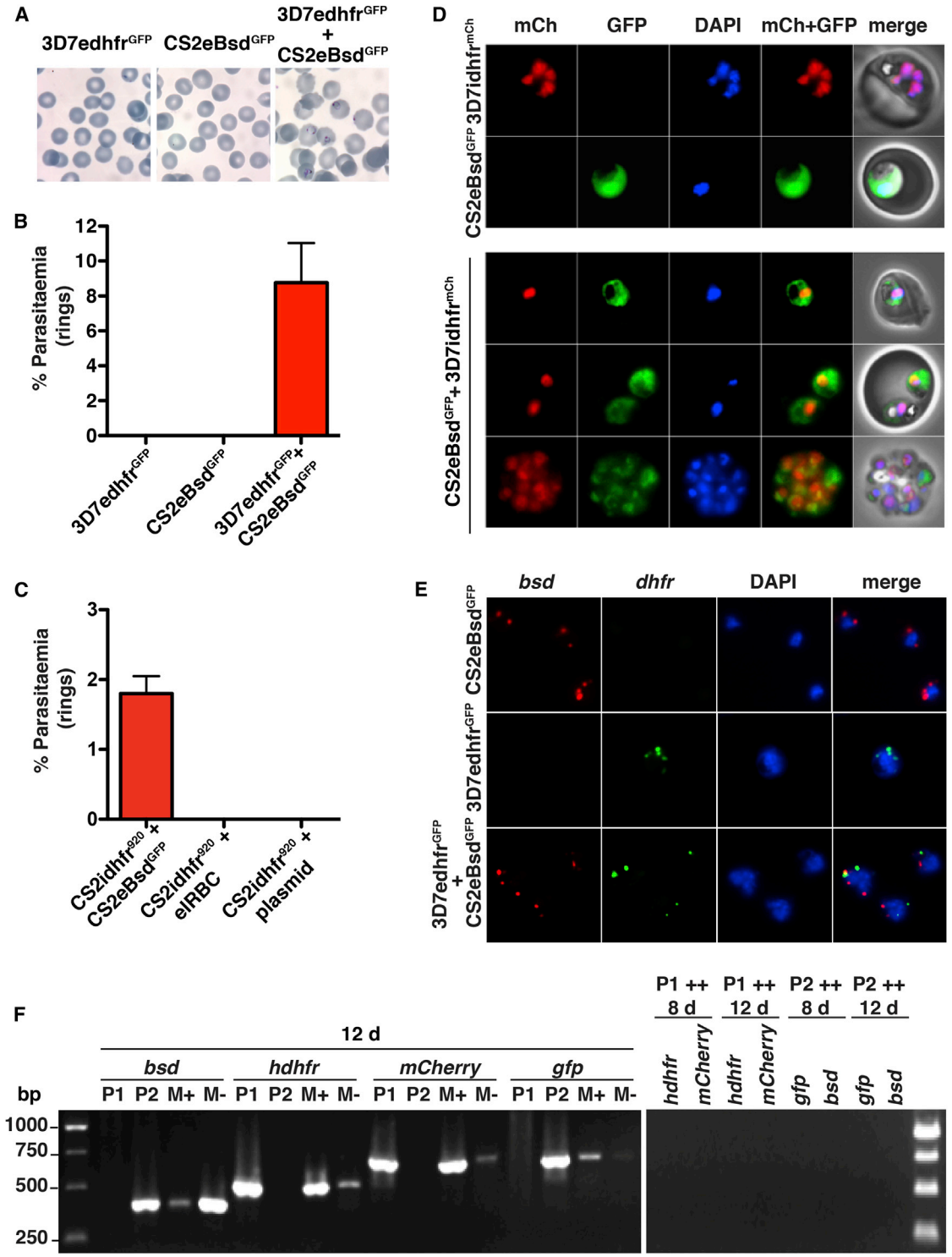

Figure 1. Communication between Parasites Results in the DNA-Dependent Transfer of Drug Resistance and Fluorescence

(A) Giemsa smears after 5 days for 3D7edhfr^{GFP} (episomal *hdhfr* gene, WR resistant) + CS2eBsd^{GFP} (episomal *blasticidin-S-deaminase* gene, Bs resistant) compared to each smear cultured alone with Bs+WR.

(B) 3D7edhfr^{GFP}+CS2eBsd^{GFP} parasites cocultured in Bs+WR and ring-stage parasitaemia determined after 5 days compared to 3D7edhfr^{GFP} and CS2eBsd^{GFP} parental controls. Scale bars represent the mean and SEM of three experiments.

(C) CS2idhfr^{920}+CS2eBsd^{GFP} coculture compared to CS2idhfr^{920} in RBCs electroporated (el) with a Bsd resistance plasmid or plasmid added to media in Bs+WR. Scale bars represent the mean and SEM of three experiments.

(legend continued on next page)

removed, and naive recipient 3D7edhfr^{GFP} was added with Bs+WR to the parasite-free medium. Remarkably, the initial presence of 3D7edhfr^{GFP}+CS2eBsd^{GFP} in the insert rescued 3D7edhfr^{GFP} growth, consistent with transfer of Bs-resistant plasmids. Moreover, there was an increase in rescue of 3D7edhfr^{GFP} associated with increasing volumes of the initial coculture (Figure 2D). Multiple experiments comparing cocultured versus single lines gave similar levels of rescue suggesting efficiency was the same (see Figure S2). These data demonstrate that stable factors are secreted into supernatants by *P. falciparum*-infected RBCs that mediate the transfer of drug resistance to other parasites.

To determine whether the dose response measured for communication activity was due to the continuous release of factor(s) between *P. falciparum* cells, we incubated ring-stage donor, CS2eBsd^{GFP}, in the insert and recipient 3D7edhfr^{GFP} in the bottom with Bs+WR (Figure 2E). The inserts were removed either immediately or between 1 and 24 hr after mixing. Increasing exposure of 3D7edhfr^{GFP} to CS2eBsd^{GFP} in inserts resulted in increased survival consistent with a greater transfer of Bs resistance. Our results demonstrate rapid and efficient plasmid transfer, even after 1 hr, maximal rescue of the 3D7edhfr^{GFP} line occurring within 10 hr of the coculture of ring stages. This suggests that *P. falciparum* employs an efficient mechanism to communicate and transfer factors harboring cellular information over long distances without direct cell-cell contact.

Communication Occurs at Ring Stages and Is Sensitive to Actin Filament and Microtubule Inhibitors

We examined the timing of communication and plasmid transfer within the blood-stage asexual cycle by the coculture of either ring or trophozoites of 3D7idhfr^{mCh}+CS2eBsd^{GFP} in Bs+WR (Figure 3A). Ring-stage coculture showed efficient plasmid transfer, whereas parasite survival for trophozoite cocultures was 10-fold less. This suggests that efficient communication and plasmid transfer occurs mainly in ring stages of the asexual life cycle.

Because drug selection of *P. falciparum* parasites causes stress and death, we addressed whether this affected cell-cell communication. Using transwells, we cocultured 3D7edhfr^{GFP}+CS2eBsd^{GFP} parasites in inserts with or without drugs for 24 hr (Figure 3B). The insert was removed, and naive 3D7edhfr^{GFP} was added to cell-free medium containing Bs+WR. In the first 24 hr, the growth of 3D7edhfr^{GFP} in wells where no drugs were initially added was greatly reduced in comparison to wells where both Bs+WR were present through experiments. Although it is suggestive of a more efficient transfer of Bs resistance during drug stress, in the absence of drugs, 3D7edhfr^{GFP}+CS2eBsd^{GFP} parasites still transferred Bs resistance to 3D7edhfr^{GFP}. Our study shows that intercellular communication between *P. falciparum*-infected RBCs occurs under normal conditions; however, signaling between cells under stress conditions, such as when faced with antimalarials in the host, is a more active process. The importance of ring stages and stress in cell-cell communication suggests that the directionality of episomal Bs plasmid transfer observed in Figures 2A and 2B may be due to Bs acting against ring stages and causing stress, whereas WR acts later and does not cause stress at the critical ring stage for cell-cell communication.

Because communication and plasmid transfer occur efficiently at ring stages without direct contact between cells, we hypothesized that EVs were providing a vectored and efficient mode of export and signaling. Given that actin and microtubules have a role in the secretion of vesicles, we tested sublethal concentrations of inhibitors of these processes for a role in *P. falciparum* communication (Dieckmann-Schuppert and Franklin, 1989; Shaw et al., 2000). Cytochalasin D (CytoD) and oryzalin (ORY) were potent inhibitors of plasmid transfer between 3D7edhfr^{GFP} and CS2eBsd^{GFP} (Figure 3C). Significant inhibition (75%) was also observed for swinholide. Both CytoD and ORY inhibition showed a dose-dependent response at sublethal levels for cocultured Bs+WR-treated parasites (Figures 3D and 3E). CytoD and ORY are inhibitors of actin polymerization and microtubule depolymerization, respectively, suggesting that these functions are required for cell-cell communication. In addition, we found that heparin blocked plasmid transfer in *P. falciparum*, which was consistent with studies showing that highly charged heparin suppresses microvesiculation (Sustar et al., 2009).

Exosome-like Vesicles Are Released into the Culture Supernatant

To address the size of mediators of *P. falciparum* cell-cell communication, we cultured CS2eBsd^{GFP} enclosed in dialysis tubing (excludes >100 kDa) with 3D7edhfr^{GFP} recipient in the outside compartment (Figure 4A). Although, in control experiments, 3D7edhfr^{GFP} grew normally when CS2eBsd^{GFP} was separated by dialysis tubing, it did not grow in the presence of Bs+WR, indicating that the mediator(s) responsible for communication was >100 kDa.

Next, we used atomic force microscopy (AFM) to determine whether EVs were present in supernatants and whether their concentration changed with differing treatments of *P. falciparum*. We visualized *P. falciparum*-infected RBCs by AFM and observed vesicles (~120 nm diameter) around parasites (Figure 4B, black arrows) as well as small protrusions on

(D) Fluorescence microscopy of live 3D7idhfr^{mCh} (mCherry) and CS2eBsd^{GFP} (GFP) cocultured. Top, 3D7idhfr^{mCh} expression of mCherry (red) in nucleus. Second panel, CS2eBsd^{GFP} expression of GFP in cytoplasm. Bottom, examples of CS2eBsd^{GFP}+3D7idhfr^{mCh} cocultures in Bs+WR after 5 days. DAPI-stained images (blue) show the nucleus and final image merged.

(E) FISH showing plasmids transferred between parasites. Top, CS2eBsd^{GFP} hybridized with *bsd* (red) and *hdhfr* (green). Middle, 3D7edhfr^{GFP} hybridized with *bsd* (red) and *hdhfr* (green). Bottom, CS2eBsd^{GFP}+3D7edhfr^{GFP} cocultured with Bs+WR and hybridized with *bsd* (red) and *hdhfr* (green). Each panel shown with DAPI-stained nuclei (blue) and merged.

(F) First panel, PCR genotyping of drug resistance (*hdhfr* and *bsd*) and fluorescent protein genes (*mCherry* and *gfp*) from 3D7idhfr^{mCh} (P1), CS2eBsd^{GFP} (P2) and 3D7idhfr^{mCh}+CS2eBsd^{GFP} in (M+) or absence (M−) of Bs+WR after 12 days. Second panel, gDNA from parental 3D7idhfr^{mCh} (P1) or CS2eBsd^{GFP} (P2) parasites in Bs+WR after 8 or 12 days.

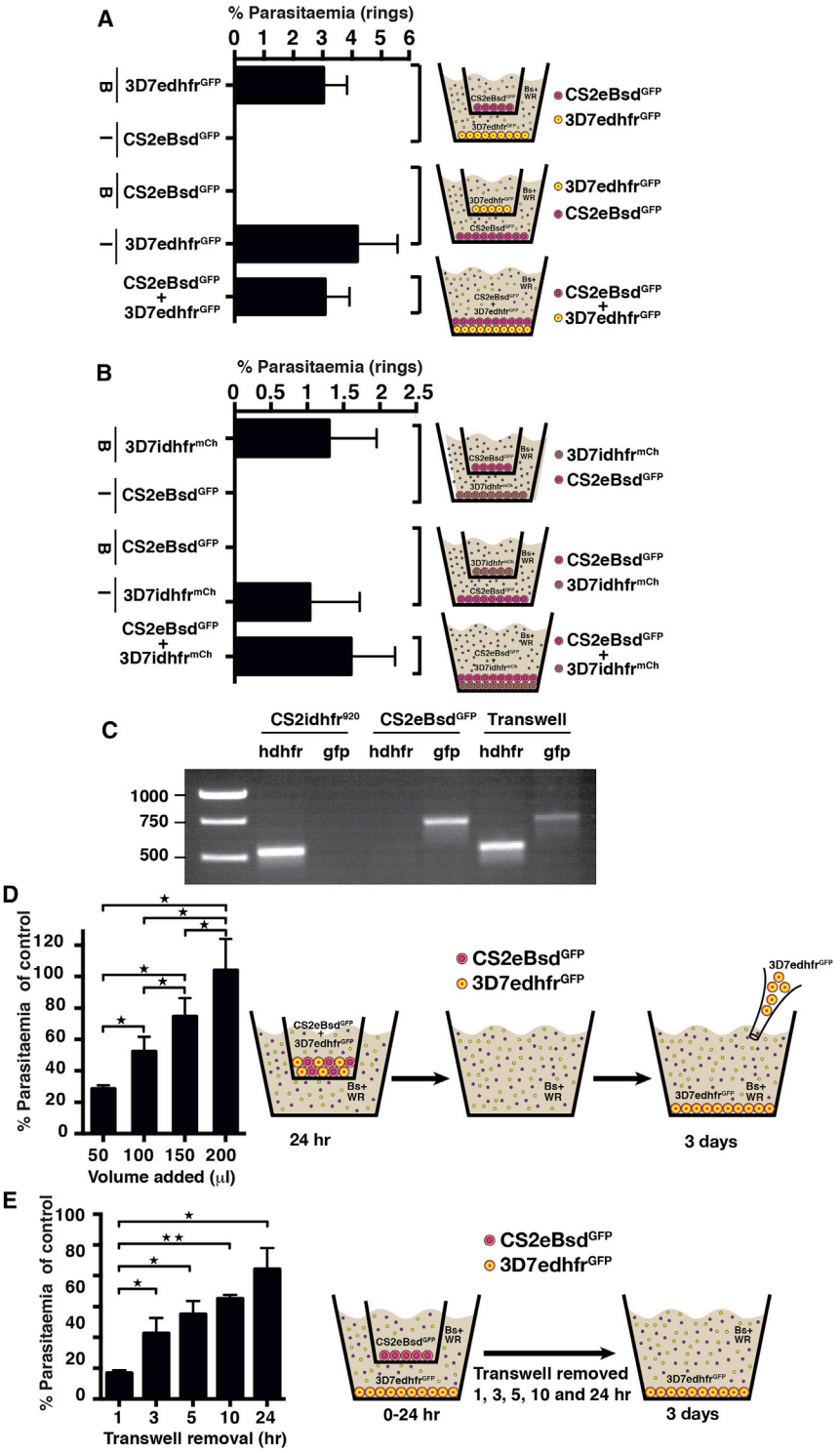

Figure 2. Parasite Communication and DNA Transfer Is Mediated by Factor(s) Released in Culture Supernatant

(A) Transwells with 3D7edhfr^{GFP} (WR resistant) and CS2eBsd^{GFP} (Bs resistant) in the insert (I) and bottom chamber (B) containing Bs+WR. Ring-stage parasitaemia was determined after 5 days in comparison to 3D7edhfr^{GFP}+CS2eBsd^{GFP}.

(B) 3D7idhfr^{mCh} (WR resistant) and CS2eBsd^{GFP} (Bs resistant) separated in insert (I) and bottom chambers (B) with Bs+WR. Ring-stage parasitaemia was determined at 5 days compared to 3D7idhfr^{mCh}+CS2eBsd^{GFP} cocultured. Scale bars represent the mean and SEM of three experiments.

(C) PCR amplification of *gfp* confirms transfer of DNA. CS2idhfr^{920} and CS2eBsd^{GFP} separated in transwells with Bs+WR compared to controls for *hDHFR* and *GFP*.

(D) Rescue of *P. falciparum* growth by cell-cell communication and plasmid transfer. Culture supernatant from 3D7edhfr^{GFP}+CS2eBsd^{GFP} (50, 100, 150, and 200 μl) in the insert rescued the growth of 3D7edhfr^{GFP} ring-stage recipient (100 μl, 1.5% parasitaemia). 3D7edhfr^{GFP} was added to the bottom chamber, and parasite survival was determined at 3 days. Scale bars represent the mean and SEM of three experiments.

See also Figures S1 and S2.

(E) Parasite communication and DNA transfer occurs within 1 hr and continues 10 hr after drug treatment. CS2eBsd^{GFP} (insert) separated from 3D7edhfr^{GFP} (bottom well) containing Bs+WR. CS2eBsd^{GFP} removed at different time points (0–24 hr) and survival of 3D7edhfr^{GFP} determined at 3 days. Scale bars represent the mean and range of two experiments. For (D) and (E), scale bars represent the mean and SEM of three experiments with differences assessed with a paired t test. *, $p \leq 0.05$; **. $p \leq 0.01$.

the RBC (Figure 4B, white arrows) that may be in the process of being released (Figure 4B). Although this was insufficient to conclude these are vesicles being actively released, it suggested that this process may occur from *P. falciparum*-infected RBCs, and we explored this in more detail.

To determine whether EVs were present in supernatant released from *P. falciparum*-infected RBCs, we incubated CS2eBsd^{GFP}+3D7edhfr^{GFP} with Bs+WR (Figure 4C, Mix++) or no drug (Figure 4C, Mix) in transwell inserts and harvested supernatants from the bottom for AFM. Remarkably, vesicles of a similar width were observed in both the presence (123.1 ± 2.08 nm) and absence (112.2 ± 17.7 nm) of drug in cell-free supernatants of CS2eBsd^{GFP}+3D7edhfr^{GFP}. Vesicle height was similar in both cases (13.1 ± 0.9 and 12.6 ± 1.6 nm, respectively). As predicted, supernatant in the absence of drugs showed that vesicles are present at lower numbers (1.5 ± 0.4 vesicles in 100 μm^2 area) in comparison to parasite mixtures in Bs+WR (8.5 ± 2.2/100 μm^2) (Figure 4C). Some vesicles appeared to be wider than the low-pass of transwell filters (400 nm) most likely because of aggregation and spreading on mica surfaces as well as AFM tip convolution

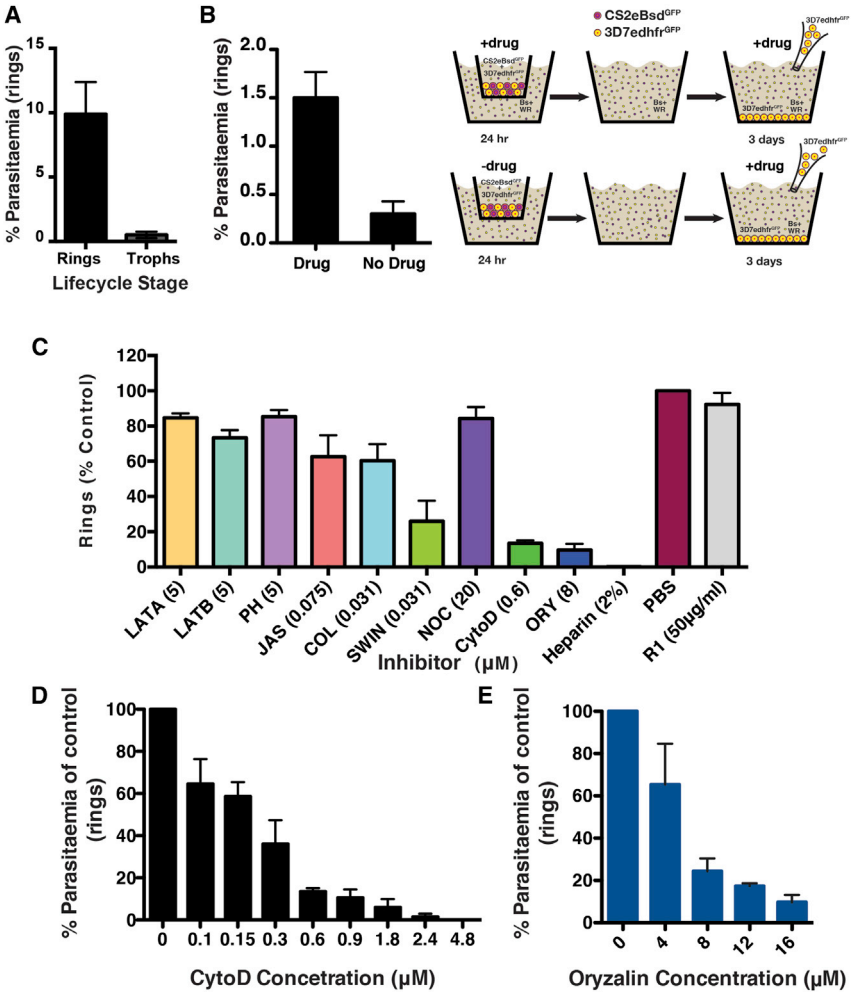

Figure 3. Actin and Microtubule Inhibitors Block Intercellular Communication in *P. falciparum*

(A) Parasite communication and plasmid transfer occurs mostly in ring stages. 3D7idhfr^{mCh}+C-S2eBsd^{GFP} were cocultured at ring or trophozoite stage and selected on Bs+WR. Ring-stage parasitaemia was counted at 5 days. Scale bars represent the mean and SEM of three experiments.

(B) Parasite communication and plasmid transfer increase under drug stress. 3D7edhfr^{GFP} and CS2Bsd^{GFP} cocultured in transwell inserts with (+drug) or without Bs+WR (−drug). After 24 hr, coculture inserts were removed, and naive 3D7edhfr^{GFP} recipient was added to the bottom transwell with fresh Bs+WR. The growth of recipient 3D7edhfr^{GFP} was assayed after 3 days. Scale bars represent the mean and SEM of four experiments.

(C) Treatment of ring-stage 3D7edhfr^{GFP}+C-S2eBsd^{GFP} parasites in Bs+WR cocultured for 20 hr with actin or microtubule inhibitors. LATA, latrunculin A; LATB, latrunculin B; PH, phalloidin; JAS, jasplakinolide; COL, cholchicine; SWIN, swinholide; NOC, nocadazole; CytoD, cytochalasin D; ORY, Oryzalin; Heparin; PBS, Phosphate buffered saline; R1, R1 peptide. Data represent ring stages expressed as percentage of a parallel non-Bs- and WR-treated control at 5 days. Subinhibitory concentrations determined from growth inhibition curves of 20 hr-treated 3D7edhfr^{GFP}+CS2eBsd^{GFP} parasites. (B) Actin inhibitor cytocholasin D and (C) the microtubule inhibitor oryzalin show dose-dependent inhibition at 5 days following 20 hr of CytoD or oryzalin treatment of 3D7edhfr^{GFP}+C-S2eBsd^{GFP} cocultures in Bs+WR. Data represent ring stages as percentage of non-Bs- and WR-treated, but cytocholasin D- or oryzalin-treated, control. Scale bars represent the mean and SEM of three experiments.

(Figure 4D). Importantly, the incubation of sublethal concentrations of communication inhibitor CytoD (Figures 3C and 3D) reduced the number of vesicles (2/100 μm^2) (width 89.73 ± 3.04 nm, height 8.1 ± 1.4 nm) (Figure 4C, Mix ++ CytoD). Vesicles were also observed in RBC supernatants (width 106.5 ± 1.12 nm, height 7.3 ± 0.6 nm), but the number was substantially less than that observed with *P. falciparum*-infected RBCs. Features of 10 to 100 nm width, with an average height of 5 nm, were observed in culture medium, which was consistent with a background deposition of protein aggregates (Figure 4C, RBC and Media). The quantity of vesicles released from *P. falciparum*-infected RBCs correlates with frequency of plasmid transfer, and this implicates vesicles as mediators of intercellular communication. The size of these vesicles suggests they are analogous to mammalian exosomes, sharing features such as release from viable cells (Bang and Thum, 2012; Record et al., 2011).

Exosome-like Vesicles Are Responsible for Cell-Cell Communication and Plasmid Transfer

In order to determine whether exosome-like vesicles, identified in culture supernatants by AFM, were responsible for cell communication and plasmid transfer, we attempted to purify them. A method employing OptiPrep density gradient centrifugation was used to fractionate the culture medium (Coleman et al., 2012). Purification of vesicles with these gradients and analysis of plasmid transfer in fractions resolved a discrete peak of activity observed in fractions 4 and 5 consistent with buoyant vesicles being responsible for plasmid transfer (Figure 5A).

We used AFM as well as negative-staining and cryo-transmission electron microscopy (cryo-TEM) to visualize contents of OptiPrep fractions. In fractions 4 and 5 a relatively homogeneous population of ~70 nm diameter spherical vesicles were observed (with AFM, sizes were: width, 70.55 ± 3.92; height, 12.37 ± 1.04) (Figures 5B and 5C). In contrast, vesicles of similar size were not present in fractions 3 and 6, although smaller aggregates of ~14 nm were observed by TEM and AFM (with AFM: width, 14.13 ± 1.37; height, 4.28 ± 0.87) as a rough background. The lack of plasmid transfer activity in fraction 3 was consistent with the smaller aggregates having no role in cell-cell communication. However, the predominance of the ~70 nm vesicles banding with cell-cell communication activity suggests that they are most likely responsible. These vesicle dimensions are

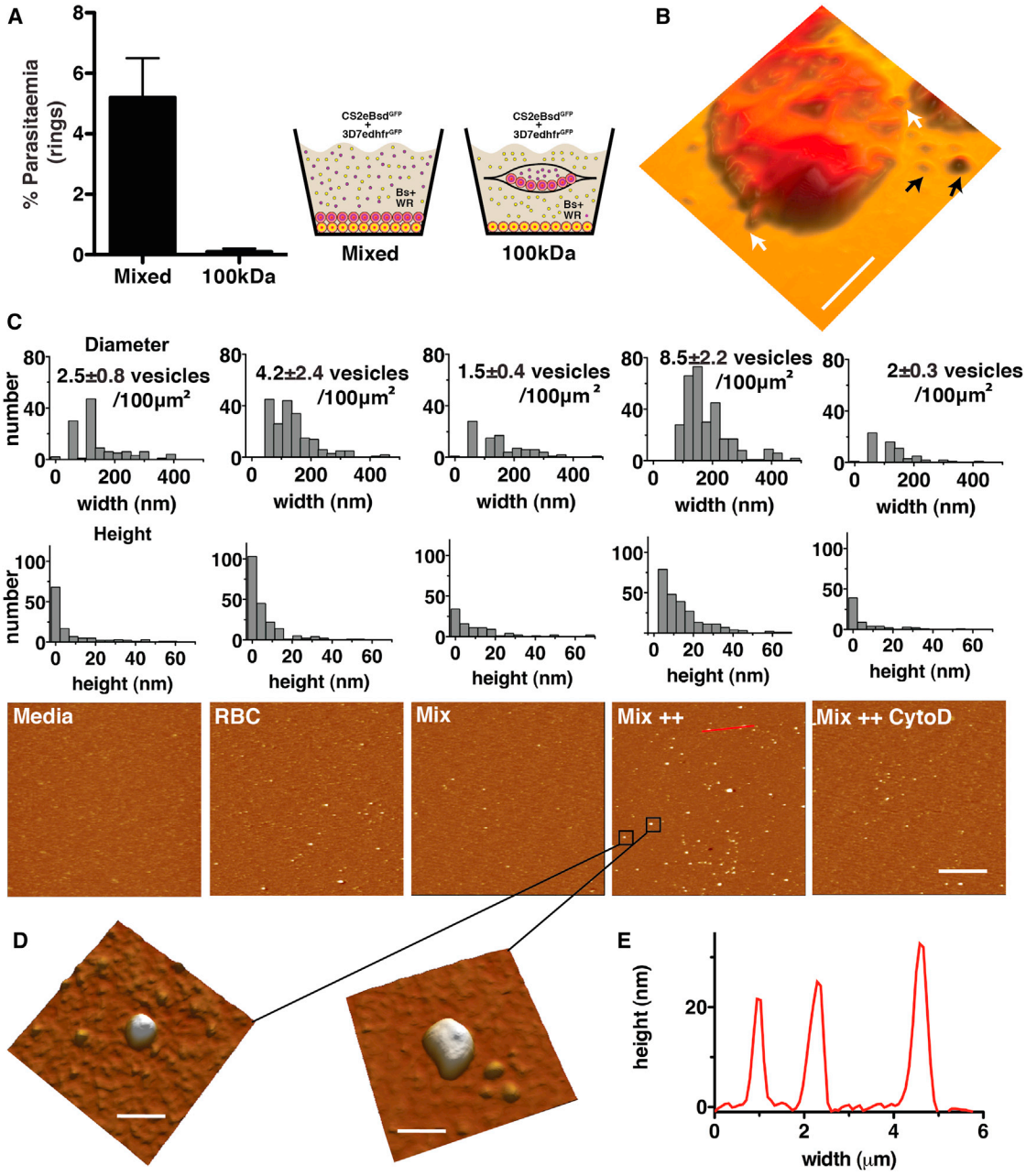

Figure 4. Visualization and Size of Vesicles from *P. falciparum*-Infected RBCs

(A) Factor(s) enabling communication between parasites are >100 kDa. Parasite communication was abolished when Bs+WR-treated 3D7edhfr^{GFP} parasites (within dish) were separated from CS2eBsd^{GFP} (within dialysis tubing). Scale bars represent the mean and range of two experiments.

(B) An AFM image of CS2 RBCs showing vesicles surrounding the cell (black arrows) and budding from cell membrane (white arrows). The scale bar represents 2 μm.

(C) AFM imaging of supernatants from media, RBCs, CS2eBsd^{GFP}+3D7edhfr^{GFP} (Mix), CS2eBsd^{GFP}+3D7edhfr^{GFP} in Bs+WR (Mix++) and CS2eBsd^{GFP}+3D7edhfr^{GFP} in Bs+WR+CytoD (Mix++CytoD). Ring-stage parasites were mixed (50/50 ratio) at same hematocrit and parasitemia. Histograms of vesicle diameter (top) and height (middle) distributions are shown. The average number and SEM of vesicles in 100 μm^2 are displayed. Data are from four independent experiments in triplicate. The scale bar represents 5 μm.

(D) AFM images of two larger vesicles (Mix ++, C). The scale bar represents 600 nm.

(E) Profile of three vesicles (red line in C, Mix ++) plotting height and diameter.

See also Table S1.

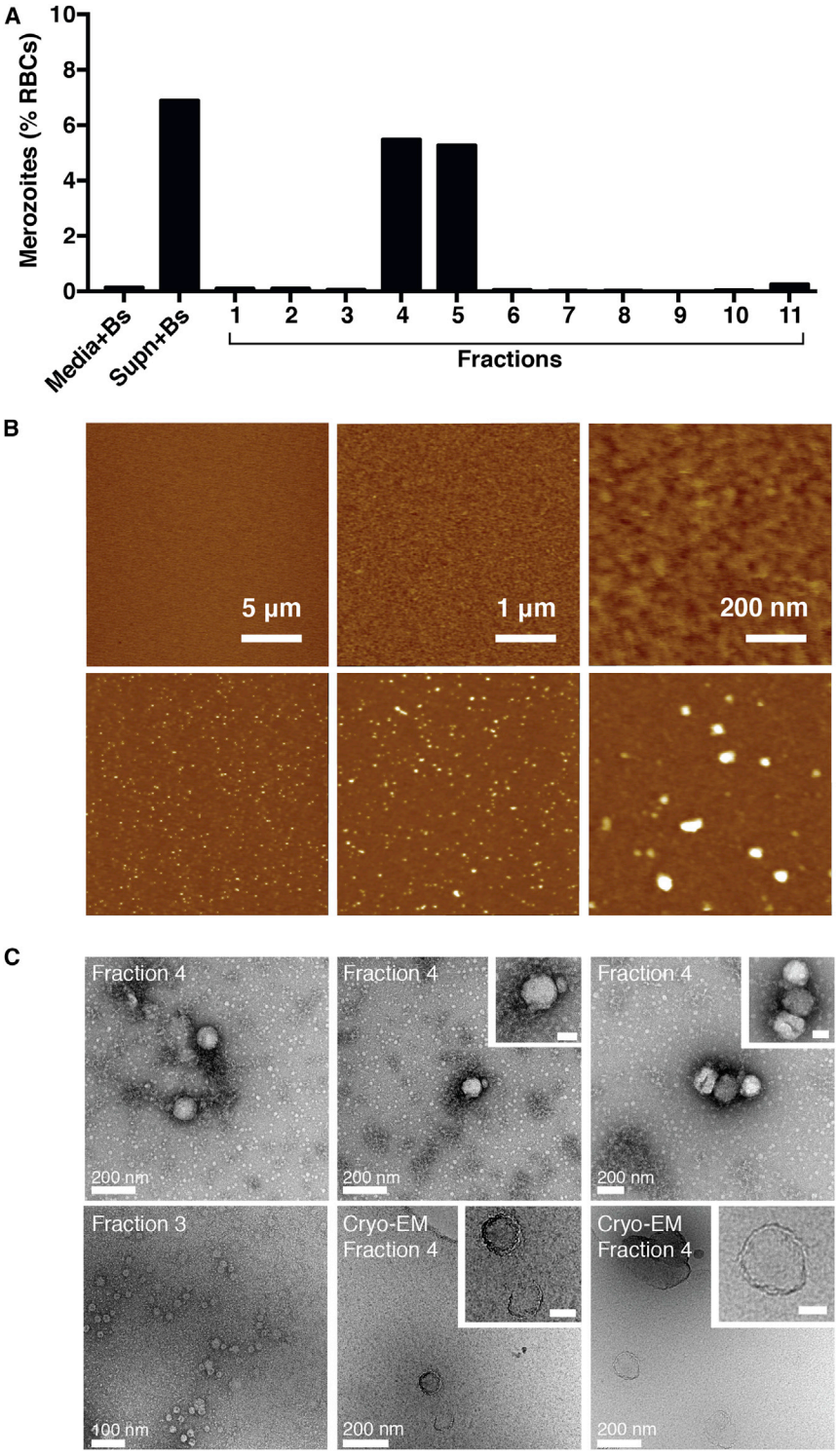

Figure 5. Purification and Communication Activity of Exosome-like Vesicles

(A) A representative experiment (of nine independent gradients) showing the purification of exosome-like vesicles with OptiPrep velocity gradient centrifugation. Communication activity of gradient fractions screened by incubating ring-stage 3D7edhfr^{GFP} with dilution series of each gradient compared to controls with media+Bs and culture supernatant+Bs. Parasite growth was assessed by comparing the number of free merozoites, expressed as a percentage of control, of newly invaded cultures between treatments.

(B) An AFM visualization of vesicles in fraction 3 (top panels) and fraction 4 (bottom panels). Size bars are shown on the top panels and are the same for the corresponding panel below.

(C) Negative-staining TEM of fraction 4 contents (top panels). In the bottom panels are negative-staining TEM of fraction 3 (left) and cryo-TEM of fraction 4 (middle and right). The inset scale bars represent 50 nm.

comparable to those observed by AFM (~120 nm diameter) when aggregation is taken into account. Altogether, these data provide strong evidence that exosome-like vesicles are responsible for cell-cell communication between *P. falciparum*-infected RBCs.

An Exported *P. falciparum* Protein Is Required for Efficient Communication

We hypothesized that *P. falciparum* proteins required for communication between parasite-infected RBCs would include those involved in trafficking to host cells. Previously, we performed a gene knockout screen and identified proteins, named PfEMP1 trafficking protein (PfPTP), required for the trafficking of virulence protein *P. falciparum* erythrocyte membrane protein 1 (PfEMP1) (Maier et al., 2008). PfEMP1 is trafficked to membranous structures called Maurer's clefts that bud from the parasitophorous vacuolar membrane, migrate to the underside of host cells, and insert into the RBC membrane (Kriek et al., 2003; Papakrivos et al., 2005). We showed that parasites CS2idhfr$^{\Delta PTP1}$, CS2idhfr$^{\Delta PTP2}$ (See also Figure S3), and CS2idhfr$^{\Delta PTP3}$ do not transfer PfEMP1 to the parasite-infected RBC surface (Maier et al., 2008). These knockout parasites were tested to determine whether they could receive a plasmid from donor CS2eBsd^{GFP}. Transfer of resistance to Bs was efficient for CS2idhfr$^{\Delta PTP1}$ and CS2idhfr$^{\Delta PTP3}$; however, it was greatly reduced for CS2idhfr$^{\Delta PTP2}$ (Figure 6A). There was no significant difference between CS2idhfr$^{\Delta PTP2}$ and CS2idhfr$^{\Delta PTP1}$ growth rates in the absence of Bs, indicating that the loss of PfPTP2 reduces cell-cell communication in coculture experiments. These experiments demonstrate that PfEMP1 is not required for efficient communication and

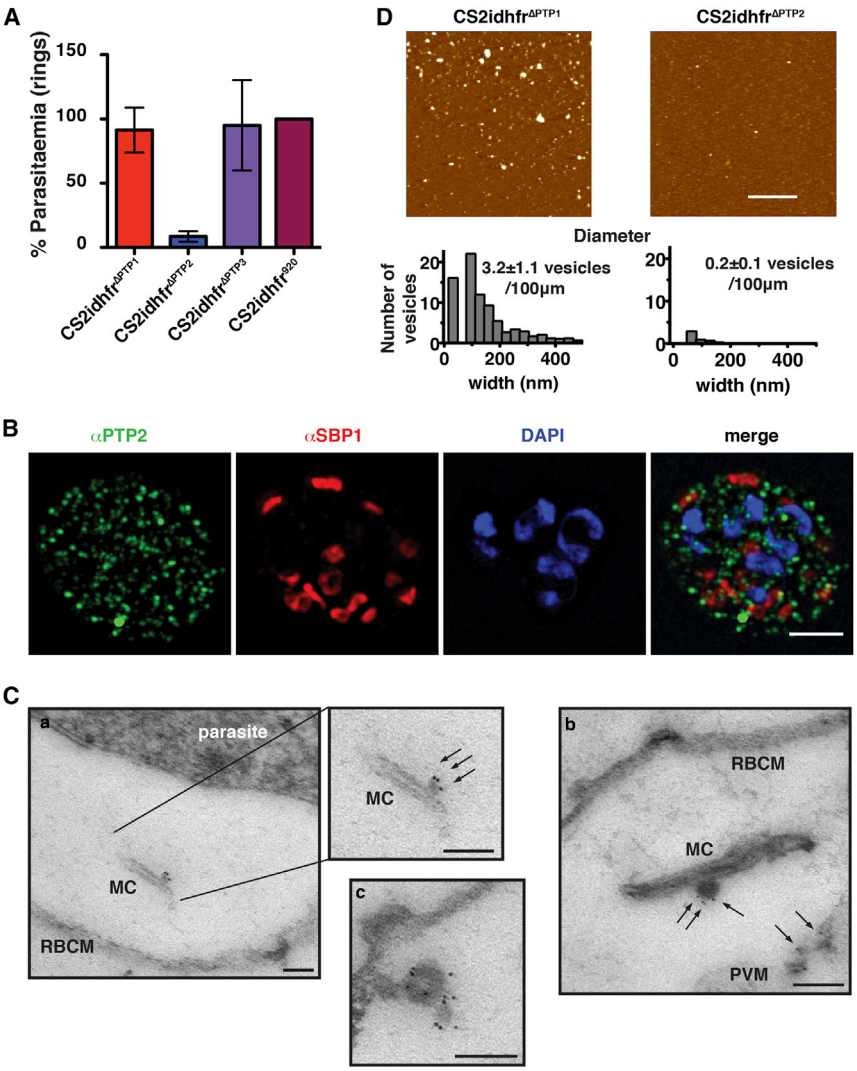

Figure 6. Communication between Parasites Is Dependent on the Maurer's Cleft Vesicle- Located Protein PfPTP2

(A) Cell-cell communication screening of *P. falciparum* knockout strains. CS2idhfr$^{\Delta PTP1}$, CS2idhfr$^{\Delta PTP2}$ (see Figure S3), and CS2idhfr$^{\Delta PTP3}$ have gene disruptions blocking PfEMP1 trafficking to parasite-infected RBCs. Knockout lines cocultured with donor CS2eBsd^{GFP} for 5 days in Bs+WR. Final parasitaemia expressed as a percentage of CS2idhfr^{920}. Scale bars represent the mean and SEM of three experiments.

(B) Localization of PfPTP2 in CS2idhfr$^{PTP2/HA}$-infected RBCs. First panel, PfPTP2 (green); second panel, SBP1 (Maurer's cleft marker; red); third panel, DAPI (blue); fourth panel, all panels merged.

(C) Immuno-EM of CS2idhfr$^{PTP2/HA}$-infected RBCs after treatment with equinotoxin II. MC, Maurer's cleft; RBCM, red blood cell plasma membrane; PVM, parasitophorous vacuole membrane. a, the side panel shows higher magnification of Maurer's cleft; arrows point to budding vesicle where PfPTP2 is localized. b, arrows point to PfPTP2 on budding vesicle and membrane material. c, an example of budding vesicle with PfPTP2 localization.

(D) A comparison of vesicle release from CS2idhfr$^{\Delta PTP1}$ and CS2idhfr$^{\Delta PTP2}$ by AFM. The quantity of vesicles released into transwell supernatants is shown in the corresponding histogram. The scale bar represents 5 μm.

See also Figure S4 and Table S2.

suggest that PfPTP2 plays a role in communication and plasmid transfer.

To address the potential roles of PfPTP2 in intercellular communication, we determined its subcellular localization using superresolution microscopy. We used CS2idhfr$^{PTP2/HA}$-infected RBCs (see Figure S3) and identified large numbers of structures in host cell cytoplasm, some of which appeared to be budding from Maurer's clefts (labeled with antibodies to skeleton binding protein 1 [SBP1]) (Figure 6B) (Maier et al., 2007). PfPTP2 was further localized to membranous structures budding from Maurer's clefts by immunoelectron microscopy, suggesting that PfPTP2-labeled material in host cell cytoplasm was derived from these membranous organelles (Figure 6C, a and inset, b, and c). The solubility of PfPTP2 was consistent with its association on the outer membrane of Maurer's clefts and vesicles, either through binding to lipid or a protein(s) in the membrane (see Figure S4). These results suggest that PfPTP2 functions in the budding of vesicles from Maurer's clefts.

Furthermore, if these cytoplasmic vesicles were the source of extracellular vesicles then CS2idhfr$^{\Delta PTP2}$ parasites, which lack the function of PfPTP2, then they would have greatly reduced quantities in the extracellular space. To examine this, we used AFM to quantitate vesicles in supernatants of CS2idhfr$^{\Delta PTP2}$ in comparison to CS2idhfr$^{\Delta PTP1}$ (Figure 6D). Indeed, CS2idhfr$^{\Delta PTP2}$ (0.2 ± 0.1 vesicles/100 μm^2, width 74.8 ± 8.3 nm) released 16-fold fewer vesicles into the supernatant than CS2idhfr$^{\Delta PTP1}$ (3.2 ± 1.1 vesicles/100 μm^2, width 76.6 ± 1.62 nm), suggesting these particles are derived from the intracellular PfPTP2-coated vesicles (Figure 6D). Moreover, this result was consistent with the significantly impaired ability of CS2idhfr$^{\Delta PTP2}$ for cell-cell communication. These data strongly suggest PfPTP2 functions in the budding of vesicles from Maurer's clefts and the release of exosome-like vesicles into supernatant, implicating *P. falciparum*'s molecular machinery in communication.

Communication between *P. falciparum* Parasites Increases Sexual Differentiation

Although it was clear that cocultured *P. falciparum* lines efficiently transfer DNA, we made the interesting observation that blood-stage parasites disappeared over 2 weeks and were replaced by increased levels of gametocytes (sexual forms). To explore whether communication between *P. falciparum* cells

promotes sexual differentiation, we determined whether gametocytes originating from cocultured 3D7idhfr^{mCh} (mCherry) and 3D7iBsd$^{CK1\text{-}GFP}$ (GFP) on Bs+WR expressed both fluorescent proteins (Figure 7A). Live fluorescence microscopy of different stages of developing gametocytes showed cytoplasmic GFP and nuclear mCherry, thus confirming the transfer of plasmids. The plasmids in these parasites are integrated via a single recombination and, consequently, can frequently loop out to reform episomal plasmids. Thus, it is likely that these have been transferred as plasmids rather than directly from a chromosomal location.

Next, we compared the quantity of gametocytes produced by 3D7edhfr^{GFP} and CS2eBsd^{GFP} when cocultured in Bs+WR. Gametocytes were quantified for 3D7edhfr^{GFP} and CS2eBsd^{GFP} cultured alone with few gametocytes observed (Figure 7B). In contrast, 17-fold more gametocytes were seen for 3D7edhfr^{GFP}+CS2eBsd^{GFP} cocultures (Figure 7B). Similar results were observed for combinations of 3D7idhfr^{mCh} and 3D7iBsd$^{CK1\text{-}GFP}$ parasites (Figure 7C). Furthermore, in a complementary approach to fully quantify gametocytogenesis, we used fluorescence-activated cell sorting analysis of Bs+WR treated 3D7edhfr^{GFP} and CS2eBsd^{GFP} parental line and cocultures with N-acetyl glucosamine (NAG) depletion of asexual, but not gametocyte, forms (Gupta et al., 1985) (Figures 7D and 7E). Again, 3D7edhfr^{GFP} and CS2eBsd^{GFP}, when cultured alone, produced low levels of gametocytes, whereas mixtures in drugs efficiently produced high levels. The 3D7idhfr/Bsd$^{\Delta 175/181}$ line, which has both *hdhfr* and *bsd* inserted into the genome (Figures 7D and 7F) (Lopaticki et al., 2011), was used as a control, and it showed that gametocyte production, although clearly evident, was much lower than in cocultured parasites. The level of conversion of Bs+WR-selected cells from surviving blood-stage parasites to gametocytes in mixed cultures was very efficient, and these experiments suggest that most, if not all, of the population that received a plasmid underwent sexual differentiation to gametocytes. These findings demonstrate that cell-cell communication between *P. falciparum* parasites allows parasite survival and increased differentiation of gametocytes for disease transmission.

DISCUSSION

Cell-cell communication and the social behavior of cells within a population have become common features in organisms ranging from higher eukaryotes to single-cell eukaryotes and bacteria (Ratajczak et al., 2006; Belting and Wittrup, 2008). This social and cooperative behavior plays an important role in many different processes ranging from cell differentiation to the development of bacterial and single-cell eukaryotic ecosystems for the enhancement of survival (Gerdes and Carvalho, 2008; Lopez et al., 2011; Marzo et al., 2012). Protozoan parasites such as *T. brucei* have a population-sensing mechanism that is important for transmission to the insect vector (MacGregor et al., 2011; Reuner et al., 1997; Vassella et al., 1997). Here, we show that *P. falciparum*-infected RBCs are capable of transferring DNA within the population via EVs that we have termed exosome-like. Importantly, these exosome-like vesicles are shed from *P. falciparum*-infected RBCs and allow parasites to transfer, receive, and propagate information that is advantageous for population growth under stressed and nonstressed conditions. Furthermore, cell-cell communication facilitates the differentiation and activation of parasites competent for transmission to mosquito vectors. Increased production of exosome-like vesicles under conditions of stress, such as drug pressure, would be highly advantageous for parasite survival in providing a means to react to environmental conditions. In other words, *P. falciparum* promotes the differentiation of sexual forms and escape to the vector in response to conditions in the host less conducive for survival.

The EVs released from *P. falciparum*-infected RBCs are termed exosome-like because they are similar in size to mammalian exosomes and share common features, such as being released from viable cells (Bang and Thum, 2012; Record et al., 2011). It is not clear whether these vesicles are the same as MPs derived by the vesiculation of RBC membranes involved in stimulation of proinflammatory responses (Couper et al., 2010), but our finding that there are subpopulations of vesicles with different sizes suggests that they may be functionally distinct. Previously, OptiPrep gradients have been used to purify exosomes from human cells and provide a method for the high-resolution separation of vesicles (Coleman et al., 2012). Using this methodology, we have shown that *P. falciparum* cell-cell communication activity was restricted to specific fractions. Visualization of the contents of fractions by AFM and electron microscopy showed that they contained spherical vesicles of ~70 nm diameter. The ability to purify these vesicles provides the opportunity for additional downstream analysis, including proteomics, lipidomics, genomics, and structural biology, to further define functional characteristics of these exosome-like vesicles.

The identification of *P. falciparum* protein PfPTP2, which plays a role in mediating intercellular communication, suggests that exosome-like vesicles may be derived from Maurer's clefts and not RBC membranes. The PfPTP2-coated particles in *P. falciparum*-infected RBCs appear to be vesicular structures, previously defined as electron-dense vesicles (EDVs), or may be related to other particles called J-dots (Hanssen et al., 2010; Külzer et al., 2010). Although the function of EDVs is unknown, their size is consistent with that observed for PfPTP2-coated structures (Hanssen et al., 2010). The localization of PfPTP2-coated vesicles in the process of budding from Maurer's clefts suggests that they are formed from these large vesicular structures that play a role in protein sorting, targeting, and packaging and, as such, have similarities to late endosomes. Whether the PfPTP2-coated vesicles are equivalent to MVBs and whether the exosome-like vesicles originate directly from them by secretion across the RBC plasma membrane remains to be determined. Disruption of PfPTP2 function decreases the number of extracellular exosome-like vesicles, and this is consistent with PfPTP2-labeled vesicles having a pivotal role in the genesis and transmission of exosome-like vesicles. However, it is also clear that PfPTP2 is important for receipt of the signal by the target cell.

The ability of *P. falciparum* to differentiate from blood-stage asexual to sexual forms is essential for transmission to mosquito vectors (reviewed in Alano, 2007). How this process is

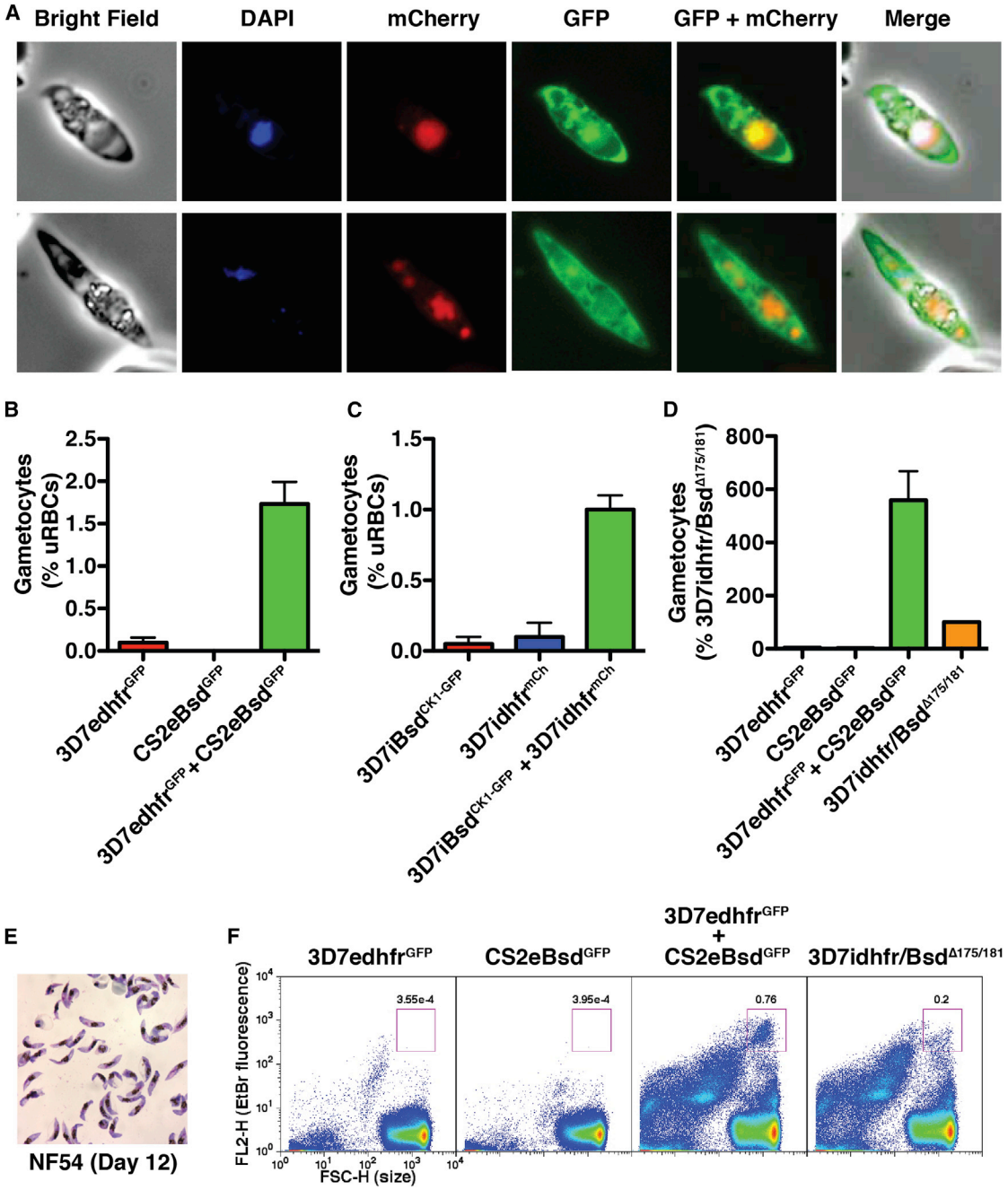

Figure 7. Communication between Parasites Results in Differentiation to Sexual Stages and Transfer of DNA

(A) Fluorescence microscopy of gametocytes produced by 3D7idhfr^{mCh}+3D7iBsd$^{CK1\text{-}GFP}$ in Bs+WR.

(B) Gametocytaemias from 3D7edhfr^{GFP} or CS2eBsd^{GFP} alone and 3D7edhfr^{GFP}+CS2eBsd^{GFP} cocultured.

(C) Gametocytaemias from 3D7iBsd$^{CK1\text{-}GFP}$ or 3D7idhfr^{mCh} alone and 3D7iBsd$^{CK1\text{-}GFP}$+3D7idhfr^{mCh} cocultured with Bs+WR. Microscopy counts expressed as percent gametocytes of uninfected RBCs.

(D) Flow cytometry of gametocytaemia for Bs+WR treated 3D7edhfr^{GFP} and CS2eBsd^{GFP} parental controls, 3D7edhfr^{GFP}+CS2eBsd^{GFP} cocultured, and 3D7idhfrBsd$^{175/181}$ double-drug-resistant control. Gametocytes measured are from 3D7edhfr^{GFP} (data not shown). Gametocytaemia for the 50/50 3D7edhfr^{GFP}+CS2eBsd^{GFP} coculture has been calculated to reflect the contribution of the 3D7edhfr^{GFP} line. Gametocytaemia is expressed as a percentage of 3D7iWRBsd$^{175/181}$ control for 200,000 RBCs. Scale bars represent the mean and SEM of three or more experiments.

(E) Giemsa smears of sorted NF54 gametocytes confirmed gating of gametocytes by flow cytometry.

(F) Representative flow cytometry plots with gated gametocyte population (square gate) for 3D7edhfr^{GFP} and CS2eBsd^{GFP} controls and 3D7edhfr^{GFP}+CS2eBsd^{GFP} coculture compared to 3D7idhfrBsd$^{175/181}$ on Bs+WR.

activated and regulated is not known. Our study demonstrates that exosome-like vesicles released from *P. falciparum*-infected RBCs enable the survival of drug-treated parasites and lead to greatly increased numbers of gametocytes competent for transmission to the next host. Intriguingly, in *T. brucei* stumpy induction factor (STI) leads to increased differentiation to the transmission-competent stumpy form at high-parasite loads (MacGregor et al., 2011; Reuner et al., 1997; Vassella et al., 1997). Here, the high levels of gametocytes achieved during cell-cell communication suggest active signaling of gametocytogenesis. This is supported by the demonstration that vesicles purified from culture supernatants act as a messenger for the induction of gametocytogenesis (Mantel et al., 2013). The exact nature of any activation signal is unknown; however, exosomes in mammalian cells are key players in signaling between cells and are known to transfer messenger RNA, microRNA, lipid mediators, and proteins (Bang and Thum, 2012; Record et al., 2011).

In summary, we have demonstrated that cell-cell communication occurs between *P. falciparum*-infected RBCs and that this provides a mechanism for increasing parasite survival in times of stress and promoting differentiation to sexual forms. This is a key advantage for parasites in maintaining infection of the human host in order to maximize the chances of transmission to the mosquito vector (MacGregor et al., 2011). Furthermore, we provide evidence that exosome-like vesicles are responsible for parasite communication. Moreover, we identified a key *P. falciparum* protein, which is for this pathway. It is likely that many other *P. falciparum* proteins are involved in the development and secretion of these vesicles in the donor cells as well as detecting the signal in the recipient. This process is potentially an excellent target for therapeutic approaches for blocking *P. falciparum* transmission to the vector and will be an important factor that requires addressing with respect to the spread of further parasite drug resistance.

EXPERIMENTAL PROCEDURES

Parasite Lines

Parasite lines are as follows: CS2eBsd^{GFP} (Ataíde et al., 2010); 3D7edhfr^{GFP} (GFP fused to PfEMP3, PF3D7_0201900) (Boddey et al., 2010); 3D7idhfr^{mCh} (mCherry fused to PF3D7_0919000) (Volz et al., 2010); 3D7iBsd$^{CK1\text{-}GFP}$ (GFP fused to CK1, PF3D7_1136500) (D. Dorin-Semblat and C. Doerig, personal communication); CS2idhfr^{920} (knockout of PFB0920w/PF3D7_0220100); CS2idhfr$^{\Delta PTP1}$, CS2idhfr$^{\Delta PTP2}$, and CS2idhfr$^{\Delta PTP3}$ (knockout of PFB0106c/PF3D7_0202200, *Pfptp1*; MAL7P1.172/PF3D7_0731100, *ptp2*, and PF14_0758/PF3D7_1478600, *ptp3*, respectively) (Maier et al., 2008); 3D7idhfr$^{175/181}$ (3D7 line with knockouts of EBA-175 and EBA-181) (Lopaticki et al., 2011); and CS2idhfr$^{PTP2/HA}$ (*Pfptp2* gene, MAL7P1.172/PF3D7_0731100, tagged with HA) (see Figure S3).

Parasite Culture and Coculture Experiments

Use of human red blood cells was approved by the Walter and Eliza Hall Human Research Ethics Committee (ethics number 86/17) and an Australian Red Cross Blood Service Agreement (11-09VIC-01). *P. falciparum* parasites were cultured in erythrocytes with routine methods. Ring-stage parasites were mixed at a 50/50 ratio between 2% to 4% hematocrit and 1% to 1.5% parasitaemia with growth (rings) counted 3 or 5 days postsetup by microscopy of Giemsa-stained thin smears. Variations on the parasite mix experiments are described in the Extended Experimental Procedures.

Electroporation of RBCs and Plasmid Addition

pHGBrHrBl-1/2 plasmid (400 μg; encodes Bsd) (Wilson et al., 2010) was added or transfected into RBCs (Fidock and Wellems, 1997) and added to cultures of trophozoite stage CS2idhfr^{920}. CS2eBsd^{GFP}+CS2idhfr^{920} parasites served as a positive control. Drugs Bs+WR (2.5 μg/ml and 5 nM, respectively) were added to rings.

Live Fluorescence and Immunofluorescence

For immunofluorescence assays, iRBCs were fixed by standard methods (Volz et al., 2012). Cells were imaged on a Zeiss Elyra PS.1 SR-SIM platform (Carl Zeiss) or a line scan confocal Zeiss LSM 5 LIVE fluorescent microscope. Structured illumination microscopy was performed on a DeltaVision OMX V4 Blaze 3D Structured Illumination Microscopy (3D-SIM) System (Applied Precision).

Fluorescent In Situ Hybridization and PCR

FISH was carried out as described previously (Volz et al., 2012). FISH experiments were visualized using a Zeiss LSM 5 LIVE fluorescent microscope.

OptiPrep Gradient Purification of Exosome-like Vesicles

Media components were fractionated by centrifugation (250, 000 × *g*, 18 hr, 4°C) through a continuous 10%–30% OptiPrep (Axis-Shield) gradient. Fractions (1 ml) were collected from the top of the gradient for further analysis.

Atomic Force Microscopy

Transwell supernatants were imaged in situ after deposition on mica surfaces. AFM images were then analyzed for number, diameter, and height (Extended Experimental Procedures).

Electron Microscopy

Magnet-purified infected RBCs were fixed in 2% paraformaldehyde and PBS, treated with Equinatoxin II (10 mg) (Anderluh et al., 1996) refixed in 2% paraformaldehyde and 0.0075% glutaraldehyde and PBS, and blocked with 1% bovine serum albumin and PBS as described previously (Jackson et al., 2007). Cells were incubated with antibody (rabbit anti-PfPTP2) and 6 nm gold-conjugated protein A (Aurion) and observed on a Phillips CM120 at 120 kV. Negative staining and cryo-TEM of purified vesicles from OptiPrep fractions was performed as described previously (Coleman et al., 2012). TEM was performed with a Tecnai G^2 F30 (FEI) transmission electron microscope operating at 300 kV (Bio21 Molecular Science and Biotechnology Institute) with defocus between 10 and 16 μm across 15,000× to 39,000× magnification.

SUPPLEMENTAL INFORMATION

Supplemental Information includes Extended Experimental Procedures, four figures, and two tables and can be found with this article online at http://dx.doi.org/10.1016/j.cell.2013.04.029.

ACKNOWLEDGMENTS

We thank the Red Cross Blood Service for erythrocytes and M. O'Neill, A. Maier, D. Dorin-Semblat, and C. Doerig for transgenic lines. We thank F. Fowkes for statistical advice and N. Dahan, M. Duffy, and J. Thompson for their advice in carrying out various assays. We thank the Advanced Microscopy Facility, Bio21 Molecular Science and Biotechnology Institute, and the Melbourne Materials Institute (MMI) for microscopy equipment. 3D-SIM was performed at the Biological Optical Microscopy Platform, University of Melbourne (http://www.microscopy.unimelb.edu.au/bomp.html). This work was supported by National Health and Medical Research Council (NHMRC) of Australia and Victorian State Government Operational Infrastructure Support and Australian Government NHMRC IRIISS. N.R.-R. is supported by a Rothschild Fellowship and the Hebrew University of Jerusalem. D.W. and N.R.-R. are supported by Early Career Fellowships from NHMRC. A.F.H. is an ARC Future Fellow and honorary NHMRC Senior Research Fellow. A.F.C. is a Howard Hughes International Scholar.

Received: December 26, 2012
Revised: March 12, 2013
Accepted: April 16, 2013
Published: May 15, 2013

REFERENCES

Alano, P. (2007). *Plasmodium falciparum* gametocytes: still many secrets of a hidden life. Mol. Microbiol. *66*, 291–302.

Anderluh, G., Pungercar, J., Strukelj, B., Macek, P., and Gubensek, F. (1996). Cloning, sequencing, and expression of equinatoxin II. Biochem. Biophys. Res. Commun. *220*, 437–442.

Ataíde, R., Hasang, W., Wilson, D.W., Beeson, J.G., Mwapasa, V., Molyneux, M.E., Meshnick, S.R., and Rogerson, S.J. (2010). Using an improved phagocytosis assay to evaluate the effect of HIV on specific antibodies to pregnancy-associated malaria. PLoS ONE *5*, e10807.

Bang, C., and Thum, T. (2012). Exosomes: new players in cell-cell communication. Int. J. Biochem. Cell Biol. *44*, 2060–2064.

Bassler, B.L., and Losick, R. (2006). Bacterially speaking. Cell *125*, 237–246.

Belting, M., and Wittrup, A. (2008). Nanotubes, exosomes, and nucleic acid-binding peptides provide novel mechanisms of intercellular communication in eukaryotic cells: implications in health and disease. J. Cell Biol. *183*, 1187–1191.

Boddey, J.A., Hodder, A.N., Günther, S., Gilson, P.R., Patsiouras, H., Kapp, E.A., Pearce, J.A., de Koning-Ward, T.F., Simpson, R.J., Crabb, B.S., and Cowman, A.F. (2010). An aspartyl protease directs malaria effector proteins to the host cell. Nature *463*, 627–631.

Campos, F.M., Franklin, B.S., Teixeira-Carvalho, A., Filho, A.L., de Paula, S.C., Fontes, C.J., Brito, C.F., and Carvalho, L.H. (2010). Augmented plasma microparticles during acute *Plasmodium vivax* infection. Malar. J. *9*, 327.

Coleman, B.M., Hanssen, E., Lawson, V.A., and Hill, A.F. (2012). Prion-infected cells regulate the release of exosomes with distinct ultrastructural features. FASEB J. *26*, 4160–4173.

Combes, V., Coltel, N., Alibert, M., van Eck, M., Raymond, C., Juhan-Vague, I., Grau, G.E., and Chimini, G. (2005). ABCA1 gene deletion protects against cerebral malaria: potential pathogenic role of microparticles in neuropathology. Am. J. Pathol. *166*, 295–302.

Couper, K.N., Barnes, T., Hafalla, J.C., Combes, V., Ryffel, B., Secher, T., Grau, G.E., Riley, E.M., and de Souza, J.B. (2010). Parasite-derived plasma microparticles contribute significantly to malaria infection-induced inflammation through potent macrophage stimulation. PLoS Pathog. *6*, e1000744.

Delabranche, X., Berger, A., Boisramé-Helms, J., and Meziani, F. (2012). Microparticles and infectious diseases. Med. Mal. Infect. *42*, 335–343.

Dieckmann, A., and Jung, A. (1986). The mechanism of pyrimethamine resistance in *Plasmodium falciparum*. Parasitology *93*, 275–278.

Dieckmann-Schuppert, A., and Franklin, R.M. (1989). Compounds binding to cytoskeletal proteins are active against *Plasmodium falciparum in vitro*. Cell Biol. Int. Rep. *13*, 207–214.

Dubey, G.P., and Ben-Yehuda, S. (2011). Intercellular nanotubes mediate bacterial communication. Cell *144*, 590–600.

Fidock, D.A., and Wellems, T.E. (1997). Transformation with human dihydrofolate reductase renders malaria parasites insensitive to WR99210 but does not affect the intrinsic activity of proguanil. Proc. Natl. Acad. Sci. USA *94*, 10931–10936.

Gerdes, H.H., and Carvalho, R.N. (2008). Intercellular transfer mediated by tunneling nanotubes. Curr. Opin. Cell Biol. *20*, 470–475.

Gupta, S.K., Schulman, S., and Vanderberg, J.P. (1985). Stage-dependent toxicity of N-acetyl-glucosamine to *Plasmodium falciparum*. J. Protozool. *32*, 91–95.

Hanssen, E., McMillan, P.J., and Tilley, L. (2010). Cellular architecture of *Plasmodium falciparum*-infected erythrocytes. Int. J. Parasitol. *40*, 1127–1135.

Jackson, K.E., Spielmann, T., Hanssen, E., Adisa, A., Separovic, F., Dixon, M.W., Trenholme, K.R., Hawthorne, P.L., Gardiner, D.L., Gilberger, T., and Tilley, L. (2007). Selective permeabilization of the host cell membrane of *Plasmodium falciparum*-infected red blood cells with streptolysin O and equinatoxin II. Biochem. J. *403*, 167–175.

Johnstone, R.M., Adam, M., Hammond, J.R., Orr, L., and Turbide, C. (1987). Vesicle formation during reticulocyte maturation. Association of plasma membrane activities with released vesicles (exosomes). J. Biol. Chem. *262*, 9412–9420.

Kriek, N., Tilley, L., Horrocks, P., Pinches, R., Elford, B.C., Ferguson, D.J., Lingelbach, K., and Newbold, C.I. (2003). Characterization of the pathway for transport of the cytoadherence-mediating protein, PfEMP1, to the host cell surface in malaria parasite-infected erythrocytes. Mol. Microbiol. *50*, 1215–1227.

Külzer, S., Rug, M., Brinkmann, K., Cannon, P., Cowman, A., Lingelbach, K., Blatch, G.L., Maier, A.G., and Przyborski, J.M. (2010). Parasite-encoded Hsp40 proteins define novel mobile structures in the cytosol of the *P. falciparum*-infected erythrocyte. Cell. Microbiol. *12*, 1398–1420.

Lopaticki, S., Maier, A.G., Thompson, J., Wilson, D.W., Tham, W.H., Triglia, T., Gout, A., Speed, T.P., Beeson, J.G., Healer, J., and Cowman, A.F. (2011). Reticulocyte and erythrocyte binding-like proteins function cooperatively in invasion of human erythrocytes by malaria parasites. Infect. Immun. *79*, 1107–1117.

Lopez, M.A., Nguyen, H.T., Oberholzer, M., and Hill, K.L. (2011). Social parasites. Curr. Opin. Microbiol. *14*, 642–648.

MacGregor, P., Savill, N.J., Hall, D., and Matthews, K.R. (2011). Transmission stages dominate trypanosome within-host dynamics during chronic infections. Cell Host Microbe *9*, 310–318.

Maier, A.G., Rug, M., O'Neill, M.T., Beeson, J.G., Marti, M., Reeder, J., and Cowman, A.F. (2007). Skeleton-binding protein 1 functions at the parasitophorous vacuole membrane to traffic PfEMP1 to the *Plasmodium falciparum*-infected erythrocyte surface. Blood *109*, 1289–1297.

Maier, A.G., Rug, M., O'Neill, M.T., Brown, M., Chakravorty, S., Szestak, T., Chesson, J., Wu, Y., Hughes, K., Coppel, R.L., et al. (2008). Exported proteins required for virulence and rigidity of *Plasmodium falciparum*-infected human erythrocytes. Cell *134*, 48–61.

Mantel, P.-Y., Hoang, A.N., Goldowitz, I., Potashnikova, D., Hamza, B., Vorobjev, I., Ghiran, I., Toner, M., Irimia, D., Ivanov, A.R., et al. (2013). Malaria microvesicles act as messengers that induce potent responses in immune cells and parasites. Cell Host Microbe *13*, 521–534.

Marzo, L., Gousset, K., and Zurzolo, C. (2012). Multifaceted roles of tunneling nanotubes in intercellular communication. Front Physiol. *3*, 72.

Nantakomol, D., Dondorp, A.M., Krudsood, S., Udomsangpetch, R., Pattanapanyasat, K., Combes, V., Grau, G.E., White, N.J., Viriyavejakul, P., Day, N.P., and Chotivanich, K. (2011). Circulating red cell-derived microparticles in human malaria. J. Infect. Dis. *203*, 700–706.

Papakrivos, J., Newbold, C.I., and Lingelbach, K. (2005). A potential novel mechanism for the insertion of a membrane protein revealed by a biochemical analysis of the *Plasmodium falciparum* cytoadherence molecule PfEMP-1. Mol. Microbiol. *55*, 1272–1284.

Ratajczak, J., Miekus, K., Kucia, M., Zhang, J., Reca, R., Dvorak, P., and Ratajczak, M.Z. (2006). Embryonic stem cell-derived microvesicles reprogram hematopoietic progenitors: evidence for horizontal transfer of mRNA and protein delivery. Leukemia *20*, 847–856.

Record, M., Subra, C., Silvente-Poirot, S., and Poirot, M. (2011). Exosomes as intercellular signalosomes and pharmacological effectors. Biochem. Pharmacol. *81*, 1171–1182.

Reuner, B., Vassella, E., Yutzy, B., and Boshart, M. (1997). Cell density triggers slender to stumpy differentiation of *Trypanosoma brucei* bloodstream forms in culture. Mol. Biochem. Parasitol. *90*, 269–280.

Rupp, I., Sologub, L., Williamson, K.C., Scheuermayer, M., Reininger, L., Doerig, C., Eksi, S., Kombila, D.U., Frank, M., and Pradel, G. (2011). Malaria parasites form filamentous cell-to-cell connections during reproduction in the mosquito midgut. Cell Res. *21*, 683–696.

Shaw, M.K., Compton, H.L., Roos, D.S., and Tilney, L.G. (2000). Microtubules, but not actin filaments, drive daughter cell budding and cell division in *Toxoplasma gondii*. J. Cell Sci. *113*, 1241–1254.

Sustar, V., Jansa, R., Frank, M., Hagerstrand, H., Krzan, M., Iglic, A., and Kralj-Iglic, V. (2009). Suppression of membrane microvesiculation—a possible anti-coagulant and anti-tumor progression effect of heparin. Blood Cells Mol. Dis. *42*, 223–227.

Vassella, E., Reuner, B., Yutzy, B., and Boshart, M. (1997). Differentiation of African trypanosomes is controlled by a density sensing mechanism which signals cell cycle arrest via the cAMP pathway. J. Cell Sci. *110*, 2661–2671.

Volz, J., Carvalho, T.G., Ralph, S.A., Gilson, P., Thompson, J., Tonkin, C.J., Langer, C., Crabb, B.S., and Cowman, A.F. (2010). Potential epigenetic regulatory proteins localise to distinct nuclear sub-compartments in *Plasmodium falciparum*. Int. J. Parasitol. *40*, 109–121.

Volz, J.C., Bártfai, R., Petter, M., Langer, C., Josling, G.A., Tsuboi, T., Schwach, F., Baum, J., Rayner, J.C., Stunnenberg, H.G., et al. (2012). PfSET10, a *Plasmodium falciparum* methyltransferase, maintains the active *var* gene in a poised state during parasite division. Cell Host Microbe *11*, 7–18.

Wilson, D.W., Crabb, B.S., and Beeson, J.G. (2010). Development of fluorescent *Plasmodium falciparum* for *in vitro* growth inhibition assays. Malar. J. *9*, 152.